Investigation on Thermodynamic Properties of a Water-Based Hematite Nanofluid

Chengzhen Wei,[†] Zhaodong Nan,*[,†] Xiaoming Wang,[†] and Zhicheng Tan[‡]

College of Chemistry and Chemical Engineering, Yangzhou University, Yangzhou 225002, P. R. China, and Thermochemistry Laboratory, Dalian Institute of Chemical Physics, Chinese Academy of Sciences, Dalian 116023, P. R. China

A friendly environmental method was used to prepare a water-based hematite (α-Fe_2O_3) nanofluid through a simple biomolecule-assisted hydrothermal process. The molar heat capacities of the obtained nanofluids, base fluids, and hematite nanoparticles were measured by a high-precision automatic adiabatic calorimeter over the temperature range of (290 to 335) K, respectively. Polynomial equations of the molar heat capacities as a function of temperature were fitted by a least-squares method for the solid and nanofluid samples. Smoothed heat capacities and thermodynamic functions of the obtained samples, such as $H(T/\mathrm{K}) - H(298.15\ \mathrm{K})$ and $S(T/\mathrm{K}) - S(298.15\ \mathrm{K})$, were calculated on the basis of the fitted polynomials and the relationships of the thermodynamic functions. On the basis of the as-obtained molar heat capacities, the excess heat capacities of the nanofluids were calculated. These excess heat capacities reveal that the stable hematite nanofluids exhibit unique properties compared with the unstable one.

Introduction

As a novel class of heat transfer fluids, nanofluids have attracted tremendous interest compared to that of traditional fluids. Since the conception of nanofluids were proposed for the first time by Choi in 1995,[1] there has been intensive research interest not only for their important applications but also for their scientific and technological importance. During the past decade, significant progress in the synthesis of nanofluids has been made, and many metallic or nonmetallic nanofluids have been achieved. It was reported that the thermal conductivity of these nanofluids was enhanced compared to base fluids.[2−10] The reasons for the thermal conductivity enhancement in nanofluids have also been investigated.[11−13] However, the thermodynamic properties of nanofluids have not been reported as far as we know.

Herein, hematite nanofluids were prepared via a simple one-step biomolecule-assisted hydrothermal route at low temperature. The molar heat capacities of the as-prepared nanofluids, base fluids, and solid hematite nanoparticles were measured by a high-precision automatic adiabatic calorimeter. On the basis of experimental results, the excess heat capacities of the nanofluids were obtained.

Materials and Methods

All of the reagents used in our experiment were of analytical grade and used without further purification. A typical experiment was as follows: 50 mL of 0.02 M L-glutamic acid aqueous solution was heated gradually to boiling. Subsequently, a certain quantity of 1.00 M $FeCl_3$ and $1.00 \cdot 10^{-2}$ M HCl mixture solution was added dropwise to the boiling L-glutamic acid aqueous solution under constant stirring and reflux for 2 h. The homogeneous solution was subsequently transferred into a stainless Teflon lined autoclave and heated at 100 °C for 48 h. The autoclave was cooled to room temperature naturally, and hematite nanofluids were obtained. The resulting solid product was centrifuged and washed successively with absolute ethanol and distilled water. The resultant hematite nanofluids are labeled as SA1, SA2, SA3, and SA4, which correspond to the various concentrations of $FeCl_3$ solution such as (0.10, 0.15, 0.20, and 0.40) M, respectively.

A high-precision automatic adiabatic calorimeter was used to determine the heat capacities of the as-prepared nanofluids, base fluids, and solid hematite nanoparticles over the temperature range of (290 to 335) K. The calorimeter was established in the Thermochemistry Laboratory of the Dalian Institute of Chemical Physics, Chinese Academy of Sciences. The principle and structure of the adiabatic calorimeter have been described in detail elsewhere.[14,15] The temperature increment was controlled to be (2 to 3) K during the whole experimental process. The mass of the solid hematite nanoparticles used for the molar heat capacity measurements was 1.43590 g, which was equivalent to 0.00899179 mol, on the basis of the corresponding molar mass of 159.690 $g \cdot mol^{-1}$. The volumes of the nanofluids and base fluids used for heat capacity measurements were about 25 mL.

Before determination of the heat capacity of the as-obtained samples, the reliability of the automatic adiabatic calorimeter was verified via measurements of the standard reference material α-Al_2O_3. On the basis of our experimental results, the deviations were within ± 0.2 % compared with the values recommended by the National Bureau of Standards over the temperature range of (80 to 400) K.[16]

Results and Discussion

The photos of the as-obtained nanofluids are presented in Figure 1. Figure 1 shows that the precipitation is found out at the bottom for the nanofluid SA4 when the as-prepared nanofluids were obtained after several minutes. The as-prepared nanofluids SA1 and SA2 are stable for about two weeks; the nanofluid SA3 is stable for about one week at ambient conditions. These obtained results demonstrate that the nanofluid becomes more stable when the concentration of $FeCl_3$ solution

* Corresponding author. Tel.: +86-514-87959896. Fax: +86-514-87959896. E-mail: zdnan@yzu.edu.cn.
[†] Yangzhou University.
[‡] Chinese Academy of Sciences.

10.1021/je900883j
Published on Web 02/01/2010

Figure 1. Photos of the as-prepared nanofluids.

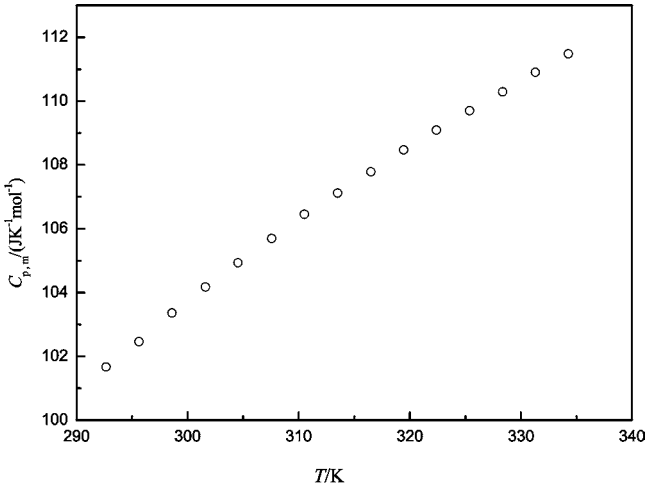

Figure 2. Curve of the experimental molar heat capacity of the as-prepared solid hematite nanoparticles as a function of temperature.

is decreased. The main reasons for the lack of stability of the nanofluid SA4 may be due to the gravity effect, because the size of the dispersed nanopaticles in nanofluid SA4 is the largest among the as-fabricated nanofluids (the images of the as-prepared solid particles investigated by transmission electron microscopy (TEM) are not shown here.).

Typical X-ray diffraction (XRD) patterns of the as-synthesized solid nanoparticles are shown in the Supporting Information. All of the reflection peaks can be indexed to pure hexagonal hematite. No other characteristic peak was detected for impurities such as β-FeOOH, Fe_3O_4, and γ-Fe_2O_3.

The experimental molar heat capacities of the as-prepared nanofluids, base fluids, and hematite nanoparticles were determined by a high-precision automatic adiabatic calorimeter over the temperature range of (290 to 335) K. The base fluids were obtained by removing the solid nanoparticles from the nanofluids. The curves of the experimental molar heat capacities to thermodynamic temperature for solid hematite nanoparticles, nanofluids, and base fluids are shown in Figures 2 and 3.

As shown in Figure 2, it is evident that the experimental molar heat capacities of the solid hematite nanoparticles increase with increasing experimental temperature. In our experiment, the experimental molar heat capacities of the as-prepared solid hematite nanoparticles are larger than those of a previous literature report.[17] The molar heat capacities of the nanofluids are larger than those of the base fluids at the same temperature as given in Figure 3. As shown in Figure 3, the molar heat capacities of the nanofluids and base fluids for SA1, SA2, and SA3 increase with increasing experimental temperature, but the values change slightly during the whole experimental temperature. The heat capacities of the as-prepared base fluids are greater than those of water obtained in our previous report.[18] However, the nanofluid SA4 has unique properties compared with the stable nanofluids, such as SA1, SA2, and SA3. The molar heat capacities for the nanofluid SA4 decrease when the experimental temperature increased. It may be related to the stability of the nanofluid. These results need to be investigated further.

The experimental molar heat capacities of the solid hematite nanoparticles and nanofluids were fitted to a polynomial equation in reduced temperature (X) via least-squares fitting.[19] The detailed results are summarized in Table 1. The smoothed molar heat capacities of the nanofluids SA1, SA2, SA3, and SA4, and the solid hematite nanoparticles were calculated on the basis of the fitted equations, respectively, and the results are listed in Table 2. The changes of the thermodynamic functions of the solid hematite nanoparticles and the nanofluids, such as ΔH and ΔS, were also calculated by the following thermodynamic equations:

$$\Delta H = H(T/\mathrm{K}) - H(298.15) = \int_{298.15}^{T} C_{p,\mathrm{m}}\,\mathrm{d}T \quad (1)$$

$$\Delta S = S(T/\mathrm{K}) - S(298.15) = \int_{298.15}^{T} \frac{C_{p,\mathrm{m}}}{T}\,\mathrm{d}T \quad (2)$$

The changes of the thermodynamic functions for the nanofluids and the solid hematite nanoparticles, such as ΔH and ΔS, which are the values of the enthalpy and entropy of the samples relative to the reference temperature of 298.15 K, are also given in Table 2 at 5 K intervals, respectively. According to Table 2, it is shown that the values of ΔS increase when the experimental temperature increased for these as-obtained samples. These results demonstrate that the molecules of the samples became more active with increasing experimental temperature.

The excess molar heat capacities for the as-obtained nanofluids were calculated via the following equation:

$$C^{\mathrm{E}}_{p,\mathrm{m}} = C_{p,\mathrm{m}} - xC_{p,\mathrm{m},1} - (1-x)C_{p,\mathrm{m},2} \quad (3)$$

where $C_{p,\mathrm{m},1}$ and $C_{p,\mathrm{m},2}$ are the experimental molar heat capacities for the as-obtained solid hematite nanoparticles and base fluids, respectively. $C_{p,\mathrm{m}}$ is the experimental molar heat capacities for the nanofluids, and x is the molar fraction of hematite nanoparticles in the nanofluids. The obtained results are displayed in Figure 4. As shown in Figure 4, it can be observed that the excess molar heat capacities of the nanofluids decrease at the beginning. When the experimental temperature is further increased, the excess molar heat capacities of the nanofluids SA1, SA2, and SA3 became about constant. However, the excess molar heat capacities of the nanofluids SA4 still decreased. From (290 to 335) K, the values of the excess molar heat capacities are all positive for SA1, SA2, and SA3. When the experimental temperature is greater than about 320 K, the values of the excess molar heat capacities become negative for the nanofluid SA4. Positive $C^{\mathrm{E}}_{p,\mathrm{m}}$ values indicated more structure in the solution.[20] The positive $C^{\mathrm{E}}_{p,\mathrm{m}}$ value indicates that the interactions between the hematite and the base fluids formed.

Influences of L-glutamic acid molecules on the stability of the nanofluid were investigated. No stable nanofluid was obtained, and the precipitation was found at once in the reaction system, when L-glutamic acid molecules were not used in the experiment. The observed results demonstrate that the action of L-glutamic acid molecules is similar as a surfactant, which promotes the stability of nanofluids.

The Brownian motion of the dispersed hematite nanoparticles in the nanofluid are enhanced when the experimental temperature is increased. Under this condition, agglomeration

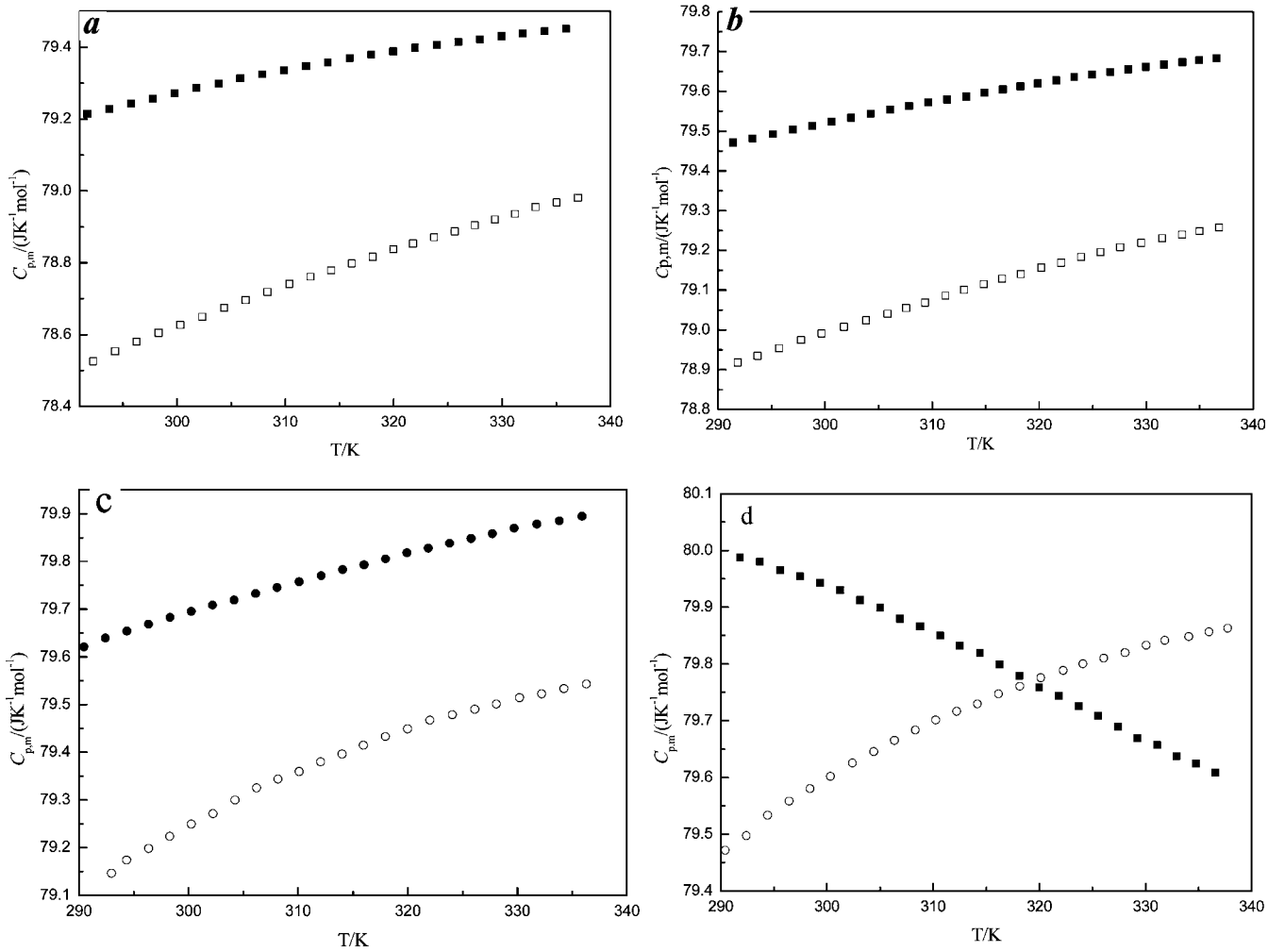

Figure 3. Curves of experimental molar heat capacities of nanofluids and base fluids as a function of temperature: (a) nanofluid SA1, (b) nanofluid SA2, (c) nanofluids SA3, (d) nanofluid SA4 (●, nanofluid; ○, base fluid).

Table 1. Polynomial Equations of the As-Prepared Solid Hematite Nanoparticles and Nanofluids

sample	polynomial equations	reduced temperature (X)	correlation coefficient (R^2)
hematite nanoparticles	$C_{p,m}/(J\cdot K^{-1}\cdot mol^{-1}) = 107.012 + 5.308X - 0.761X^2 + 0.338X^3 - 0.105X^4 - 0.191X^5$	$(T/K-313)/23$	0.99996
SA1	$C_{p,m}/(J\cdot K^{-1}\cdot mol^{-1}) = 79.354 + 0.123X - 0.033X^2 + 0.008X^3 + 0.005X^4 - 0.006X^5$	$(T/K-313)/23$	0.99996
SA2	$C_{p,m}/(J\cdot K^{-1}\cdot mol^{-1}) = 79.593 + 0.110X - 0.014X^2 - 0.002X^3 - 0.003X^4 - 0.001X^5$	$(T/K-314)/23$	0.99995
SA3	$C_{p,m}/(J\cdot K^{-1}\cdot mol^{-1}) = 79.776 + 0.142X - 0.006X^2 - 0.014X^3 - 0.013X^4 + 0.011X^5$	$(T/K-313)/23$	0.99992
SA4	$C_{p,m}/(J\cdot K^{-1}\cdot mol^{-1}) = 79.819 - 0.214X - 0.026X^2 + 0.014X^3 + 0.007X^4 + 0.008X^5$	$(T/K-314)/23$	0.99981

of hematite nanoparticles could easily form, which leads the excess heat capacities to decrease. It is generally accepted that the agglomeration results in settlement. From Figure 4, it is found that the excess heat capacities for the as-prepared nanofluids SA1, SA2, and SA3 are about constant when the experimental temperature is increased from (325 to 335) K. The results indicate that the agglomeration of the as-obtained hematite nanoparticles in the nanofluids would not continue and could not lead to precipitation. Compared with the stable nanofluids, the unstable nanofluid SA4 exhibits unique properties. The excess heat capacity decreased from positive to negative as the experimental temperature increased. From these results, we can infer that the agglomeration of the hematite nanoparticles would be formed, and result in settlement with increasing experimental temperature for SA4. To confirm the experimental results, the nanofluids SA3 and SA4 were heated to about 340 K. No precipitation was found for the nanofluid SA3. However, precipitation was found for the nanofluid SA4. The solid hematite nanoparticles were obtained by centrifugation of the nanofluids SA3 and SA4, and TEM images of the as-obtained solid hematite nanoparticles are shown in the Supporting Information. It is clearly found that the agglomeration of hematite nanoparticles was insignificant for the nanofluid SA3. However, the aggregation of hematite nanoparticles is obvious for the nanofluids SA4. These observed results are in agreement with those observed by calorimetry.

Conclusions

In summary, we have presented a simple biomolecule-assisted hydrothermal route to prepare hematite (α-Fe_2O_3) nanofluids

Table 2. Smoothed Heat Capacities and Thermodynamic Functions of the As-Prepared Solid Hematite Nanoparticles and Nanofluids

T	$C_{p,m}$	ΔH	ΔS
K	$J \cdot K^{-1} \cdot mol^{-1}$	$J \cdot mol^{-1}$	$J \cdot K^{-1} \cdot mol^{-1}$
	Hematite Nanoparticles		
290	100.90	−0.832	−2.829
295	102.33	−0.324	−1.092
300	103.73	0.191	0.640
305	105.06	0.713	2.366
310	106.31	1.242	4.084
315	107.47	1.776	5.795
320	108.57	2.316	7.496
325	109.62	2.862	9.817
330	110.64	2.413	10.869
335	111.62	3.968	12.540
298.15	103.22	0.000	0.000
	SA1		
290	79.20	−0.646	−2.196
295	79.24	−0.250	−0.842
300	79.27	0.147	0.490
305	79.31	0.543	1.801
310	79.34	0.940	3.091
315	79.36	1.336	4.360
320	79.39	1.733	5.611
325	79.41	2.130	6.842
330	79.43	2.527	8.054
335	79.45	2.925	9.249
298.15	79.26	0.000	0.000
	SA2		
290	79.46	−0.648	−2.203
295	79.49	−0.250	−0.844
300	79.52	0.147	0.492
305	79.55	0.545	1.807
310	79.57	0.943	3.100
315	79.60	1.341	4.374
320	79.62	1.739	5.627
325	79.64	2.137	6.862
330	79.66	2.535	8.054
335	79.68	2.933	8.078
298.15	79.51	0.000	0.000
	SA3		
290	79.62	−0.649	−2.208
295	79.66	−0.251	−0.846
300	79.69	0.147	0.493
305	79.73	0.546	1.810
310	79.76	0.945	3.107
315	79.79	1.344	4.383
320	79.82	1.743	5.640
325	79.84	2.142	6.878
330	79.87	2.541	8.097
335	79.89	2.941	9.298
298.15	79.68	0	0
	SA4		
290	80.00	−0.652	−2.217
295	79.97	−0.252	−0.849
300	79.94	0.148	0.495
305	79.90	0.547	1.815
310	79.86	0.947	3.114
315	79.81	1.346	4.392
320	79.76	1.745	5.648
325	79.71	2.144	6.884
330	79.66	2.542	8.101
335	79.62	2.940	9.299
298.15	79.95	0	0

at low temperature. No surfactant was used in the whole fabrication process. The experimental molar heat capacities of the as-obtained nanofluids, base fluids, and solid hematite nanoparticles were measured. The thermodynamic functions were also calculated. On the basis of the as-obtained molar heat capacities, the excess heat capacities for the as-prepared nanofluid samples were calculated. The results show that the stable hematite nanofluids exhibit different properties compared with the unstable nanofluid.

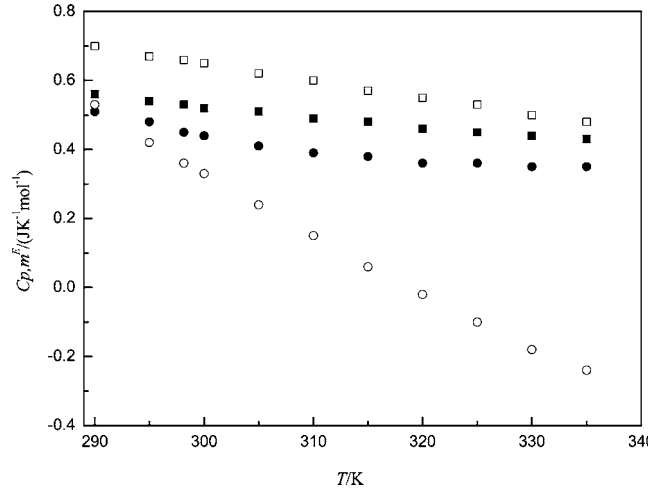

Figure 4. Excess molar heat capacity of the as-obtained nanofluids at different temperatures: □, SA1; ■, SA2; ●, SA3; and ○, SA4.

Supporting Information Available:

XRD patterns of the solid α-Fe_2O_3 nanoparticles obtained from different nanofluids and TEM images of the as-obtained solid hematite nanoparticles from the heated nanofluid samples. This material is available free of charge via the Internet at http://pubs.acs.org.

Literature Cited

(1) Choi, S. U. S. Enhancing Thermal Conductivity of Fluid with Nanoparticles. *ASME Pap.* **1995**, *231*, 99–105.
(2) Zhu, H. T.; Zhang, C. Y.; Tang, Y. M.; Wang, J. X.; Ren, B.; Yin, Y. S. Preparation of Carbon Nanotube-supported Palladium Nanoparticles by Self-regulated Reduction of Surfactant. *Carbon* **2007**, *45*, 203–206.
(3) Eastman, J. A.; Choi, S. U. S.; Li, S.; Yu, W.; Thompson, L. J. Anomalously Increased Effective Thermal Conductivities of Ethylene Glycol-based Nanofluids Containing Copper Nanoparticles. *Appl. Phys. Lett.* **2001**, *78*, 718–720.
(4) Jang, S. P.; Choi, S. U. S. Role of Brownian Motion in the Enhanced Thermal Conductivity of Nanofluids. *Appl. Phys. Lett.* **2004**, *84*, 4316–4318.
(5) Xue, Q.; Xu, W. M. A Model of Thermal Conductivity of Nanofluids with Interfacial Shells. *Mater. Chem. Phys.* **2005**, *90*, 298–301.
(6) Li, X. F.; Zhu, D. S.; Wang, X. J.; Wang, N.; Gao, J. W.; Li, H. Thermal Conductivity Enhancement Dependent pH and Chemical Surfactant for Cu-H_2O Nanofluids. *Thermochim. Acta* **2008**, *469*, 98–103.
(7) Xuan, Y.; Li, Q. Heat Transfer Enhancement of Nanofluids. *Int. J. Heat Fluid Flow* **2000**, *21*, 58–64.
(8) Zhu, H. T.; Lin, Y. S.; Yin, Y. S. A Novel One-step Chemical Method for Preparation of Copper Nanofluids. *J. Colloid Interface Sci.* **2004**, *277*, 100–103.
(9) Zhu, H. T.; Zhang, C. Y.; Tang, Y. M.; Wang, J. X. Novel Synthesis and Thermal Conductivity of CuO Nanofluid. *J. Phys. Chem. C* **2007**, *111*, 1646–1650.
(10) Lee, S.; Choi, S. U. S.; Li, S.; Eastman, J. A. Measuring Thermal Conductivity of Fluids Containing Oxide Nanoparticles. *J. Heat Transfer* **1999**, *121*, 280–289.
(11) Kumar, D. H.; Patel, H. E.; Kumar, V. R. R.; Sundararajan, T.; Pradeep, T.; Das, S. K. Model for Heat Conduction in Nanofluids. *Phys. Rev. Lett.* **2004**, *93*, 144301–144304.
(12) Vadasz, P.; Vadasz, P. Heat Conduction in Nanofluid Suspensions. *J. Heat Transfer* **2006**, *128*, 465–477.
(13) Keblinski, P.; Phillpot, S. R.; Choi, S. U. S.; Eastman, J. A. Mechanisms of Heat Flow in Suspensions of Nano-sized Particles (Nanofluids). *Int. J. Heat Mass Transfer* **2002**, *45*, 855–863.
(14) Tan, Z. C.; Sun, L. X.; Meng, S. H.; Li, L.; Zhang, J. B. Heat Capacities and Thermodynamic Functions of P-chlorobenzoic Acid. *J. Chem. Thermodyn.* **2002**, *34*, 1417–1429.
(15) Nan, Z.; Wei, C.; Yang, Q.; Tan, Z. C. Thermodynamic Properties of Carbon Nanotubes. *J. Chem. Eng. Data* **2009**, *54*, 1367–1370.

(16) Ditmars, D. A.; Ishihara, S.; Chang, S. S.; Bernstein, G.; West, E. D. Enthalpy and Heat-Capacity Standard Reference Material: Synthetic Sapphire (α-Al_2O_3) from 10 to 2250 K. *J. Res. Natl. Bur. Stand.* **1982**, *87*, 159–163.
(17) Touloukian, Y. S.; Buyco, E. H. *Thermophysical Properties of Matter, Specific Heat, Nonmetallic Solids*; IFI/Plenum: New York, 1970; Vol. 5, p 110.
(18) Nan, Z.; Lan, X. Z.; Sun, L. X.; Tan, Z. C. Thermodynamic Investigation of Crystalline $K_2Cr_2O_7$ and Aqueous $K_2Cr_2O_7$ Solution. *Int. J. Therm. Sci.* **2003**, *42*, 657–664.
(19) Nan, Z.; Tan, Z. C. Thermodynamic Investigation of the Azeotropic Binary Mixture Water + *n*-Propanol. *J. Chem. Eng. Data* **2005**, *50*, 6–10.
(20) Cerdeirina, C. A.; Tovar, C. A.; Carballo, E.; Romani, L.; Delgado, M. C.; Torres, L. A.; Costas, M. Temperature Dependence of the Excess Molar Heat Capacities for Alcohol-Alkane Mixtures. Experimental Testing of the Predictions from a Two-State Model. *J. Phys. Chem. B* **2002**, *106*, 185–191.

Received for review October 25, 2009. Accepted January 14, 2010. The financial support from the National Science Foundation of China (20753002) and the Natural & Scientific Grant of Jiangsu Province (BK2009181), China, is gratefully acknowledged.

JE900883J